Electrospray Mass Spectrometry and Fragmentation of N-Linked Carbohydrates Derivatized at the Reducing Terminus

ARTICLE *in* JOURNAL OF THE AMERICAN SOCIETY FOR MASS SPECTROMETRY · NOVEMBER 2000

Impact Factor: 2.95 · DOI: 10.1016/S1044-0305(00)00156-2 · Source: PubMed

1 AUTHOR:

David John Harvey
University of Oxford
402 PUBLICATIONS **13,103** CITATIONS

SEE PROFILE

Electrospray Mass Spectrometry and Fragmentation of N-Linked Carbohydrates Derivatized at the Reducing Terminus

David J. Harvey
Department of Biochemistry, Oxford Glycobiology Institute, Oxford, United Kingdom

Derivatives were prepared from N-linked glycans by reductive amination from 2-aminobenzamide, 2-aminopyridine, 3-aminoquinoline, 2-aminoacridone, 4-amino-*N*-(2-diethylaminoethyl)benzamide, and the methyl, ethyl, and butyl esters of 4-aminobenzoic acid. Their electrospray and collision-induced dissociation (CID) fragmentation spectra were examined with a Q-TOF mass spectrometer. The strongest signals were obtained from the $[M + Na]^+$ ions for all derivatives except sugars derivatized with 4-amino-*N*-(2-diethylaminoethyl)benzamide which gave very strong doubly charged $[M + H + Na]^{2+}$ ions. The strongest $[M + Na]^+$ ion signals were obtained from the butyl ester of 4-aminobenzoic acid and the weakest from 2-aminopyridine. The most informative spectra were recorded from the $[M + Li]^+$ or $[M + Na]^+$ ions. These spectra were dominated by ions produced by sequence-revealing glycosidic cleavages and "internal" fragments. Linkage-revealing cross-ring cleavage ions were reasonably abundant, particularly from high-mannose glycans. Although the nature of the derivative was found to have little effect upon the fragmentation pattern, 3-aminoquinoline derivatives gave marginally more abundant cross-ring fragments than the other derivatives. $[M + H]^+$ ions formed only glycosidic fragments with few, if any, cross-ring cleavage ions. Doubly charged molecular ions gave less informative spectra; singly charged fragments were weak, and molecular ions containing hydrogen ($[M + 2H]^{2+}$ and $[M + H + Na]^{2+}$) fragmented as the $[M + H]^+$ singly charged ions with no significant cross-ring cleavages. (J Am Soc Mass Spectrom 2000, 11, 900–915) © 2000 American Society for Mass Spectrometry

Most carbohydrates are difficult to detect when analyzed by techniques such as high-performance liquid chromatography (HPLC) because they lack a chromophore. Consequently, it is common practice to form a derivative at the reducing terminus to enable the compounds to be detected by UV absorption or fluorescence. The most common derivatization technique is reductive amination involving condensation of the ring-opened (carbonyl) form of the carbohydrate with an amine, usually aromatic. The resulting Schiff base is comparatively unstable and is reduced to the corresponding secondary amine. All stages of the derivatization can conveniently be performed in a single reaction.

Several amines have been used in this context and a number of these have also been investigated as derivatives for improving mass spectrometric detection limits and fragmentation over that produced by the native carbohydrates. Many of these derivatives have been discussed in a recent review [1]. For example, Poulter and Burlingame [2] investigated a series of alkyl-4-aminobenzoates of linear and N-linked glycans, ionized by fast-atom bombardment (FAB), and found that sensitivity increased with chain length with optimal results being obtained with the *n*-octyl ester. Informative negative ion spectra were obtained. Takao et al. [3] have used the 2-(diethylamino)ethyl ester of 4-aminobenzoic acid (ABDEAE) to prepare derivatives of maltoheptaose, dextran, and the N-linked glycan, $(GlcNAc)_2(Man)_8$ and have reported sensitivity increases of 1000-fold over that of the free glycan when the derivatives were examined by matrix-assisted laser desorption/ionization (MALDI) mass spectrometry. An $[M + H]^+$ ion rather than the more normal $[M + Na]^+$ ion was formed from the tertiary amine function and probably accounted for the gain in ion yield. Sensitivity increases on a smaller scale have been reported for other derivatives such as those prepared from 2-aminopyridine (2-AP, amine 2, Table 1) [4–8], 4-aminobenzoic acid ethyl ester (ABEE, amine 6, Table 1) [8], and 4-trimethylaminoaniline [trimethyl-(4-aminophenyl) amino or TMAPA derivatives] [8–10]. Derivatives prepared from 2-aminobenzamide (2-AB, amine 1, Table 1) currently appear to be the most popular for conferring fluorescence to glycans for HPLC detection [11], even though the related 2-aminobenzoic acid (2-AA) derivatives have been reported to provide greater fluorescence [12]. The latter derivatives gave excellent negative

Address reprint requests to Dr. David J. Harvey, Oxford Glycobiology Institute, Department of Biochemistry, South Parks Road, Oxford, OX1 3QU, UK. E-mail: dh@glycob.ox.ac.uk

1044-0305/00/$20.00
PII S1044-0305(00)00156-2

Received March 1, 2000
Revised June 5, 2000
Accepted June 8, 2000

Table 1. Structures of the amines used for the preparation of derivatives

No.	Amine	Abbreviation	Mass Increment	Structure
1	2-Aminobenzamide	2-AB	120	
2	2-Aminopyridine	2-AP	78	
3	2-Aminoacridone	2-AMAC	194	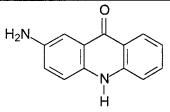
4	3-Aminoquinoline	3-AQ	128	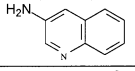
5	4-Aminobenzoic acid methyl ester	ABME	135	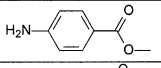
6	4-Aminobenzoic acid ethyl ester	ABEE	149	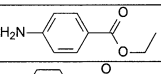
7	4-Aminobenzoic acid n-butyl ester	ABBE	176	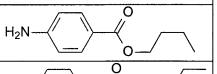
8	4-amino-N-(2-diethylaminoethyl)benzamide	DEAEAB	219	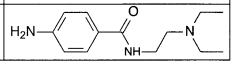

ion MALDI spectra and enable neutral glycans to be examined in the negative ion mode as $[M - H]^-$ ions. Fragmentation of the 2-AB derivatives of neutral N-linked glycans has recently been described [13].

Several recent papers have reported derivatization with 2-aminoacridone (2-AMAC, amine 3, Table 1) [14–21] for use with both MALDI and electrospray. The derivatives gave strong MALDI spectra that contained $[M + H]^+$ in addition to $[M + Na]^+$ and $[M + K]^+$ ions and, under electrospray conditions, gave $[M + H + Na]^{2+}$ and $[M + 2H]^{2+}$ ions. The latter ions have been shown to give informative CID spectra when examined with a Q-TOF instrument. A recent development by these investigators has been the introduction of 3-(acetylamino)-6-aminoacridine which was claimed to possess higher fluorescence than 2-AMAC and to enable N-linked glycans to be examined by capillary electrophoresis/electrospray mass spectrometry [22].

A few investigators have dispensed with the reductive stage in the derivatization reaction and have examined the carbonyl condensation products directly. Thus, Naven and Harvey [23] used Girard's T reagent whose cationic site gave an increase in sensitivity of 10-fold under electrospray conditions. Zhao et al. [24] have used substituted-oxime formation for adding a basic peptide residue to the reducing terminus of several neutral N-linked glycans, and have reported sensitivity increases of between 50- and 1000-fold by MALDI.

In this laboratory, glycans are usually examined either as the native compounds or as 2-AB derivatives. We have shown that the free glycans, ionized as their sodium adducts, give large numbers of diagnostic fragment ions when examined by CID on a Q-TOF instrument [25] but the effect of different derivatives on mass spectrometric sensitivity and fragmentation has not been systematically studied.

Complex sugars generally fragment to give four types of ions. The major ions are usually the result of glycosidic cleavages where bond rupture occurs between the sugar rings and involves a hydrogen migration. Cross-ring cleavages, involving the rupture of two bonds from a sugar ring, are generally weaker and are not seen under all conditions. The other major ions are "internal fragments" resulting from losses, either glycosidic or cross-ring, from several sites in the molecule. Sugars ionized by metal attachment also give a metal cation. The accepted nomenclature for describing these fragment ions is that proposed by Domon and Costello in 1988 [26].

Glycosidic cleavages provide information on constituent monosaccharide sequence and branching, whereas cross-ring cleavages can be used to define linkage. These latter ions are usually more prominent in the spectra of lithium, sodium, and potassium adducts than in those of the spectra of protonated molecular ions [27]. They are generally weak when compared with the abundance of the glycosidic cleavage ions [28] unless CID spectra are recorded at high collision energies [29, 30]. Their relative abundance appears to be highest in the spectra of glycans ionized as lithium adducts [27], the use of which has provided linkage information on a range of glycans [31, 32]. Cross-ring fragments from the decomposition of sodiated ions generated from either free or permethylated glycans have been used by numerous investigators for obtaining information on linkage from many types of carbohydrate (see, for example, [2, 33, 34]).

In this paper, we report the preparation and comparative electrospray and MALDI detection sensitivity of a number of these derivatives, listed in Table 1, and the effect of these derivatives on the subsequent CID fragmentation.

Materials and Methods

N-linked glycans were obtained from Oxford GlycoSciences (Abingdon, Oxfordshire, UK) or were released from glycoproteins (obtained from Sigma Chemical, Poole, Dorset, UK) with hydrazine [35]. The primary amines, 2-aminobenzamide (2-AB), 2-aminopyridine (2-AP), 3-aminoquinoline (3-AQ), 2-aminoacridone (2-AMAC), 4-amino-*N*-(2-diethylaminoethyl)benzamide hydrochloride (procainamide, 4-DEAEAB), and the methyl (ABME), ethyl (ABEE), and butyl (ABBE) esters of 4-aminobenzoic acid were purchased from Aldrich Chemical (Poole, Dorset, UK). The MALDI matrix 2,5-dihydroxybenzoic acid (DHB) was also purchased from Aldrich and used without further purification.

Preparation of Derivatives

Derivatives prepared by reductive amination. These compounds were prepared essentially by the method described by Prime et al. [36]. Briefly, the dried glycan (100 pmol–10 nmol) was dissolved in dry DMSO (6 μL)

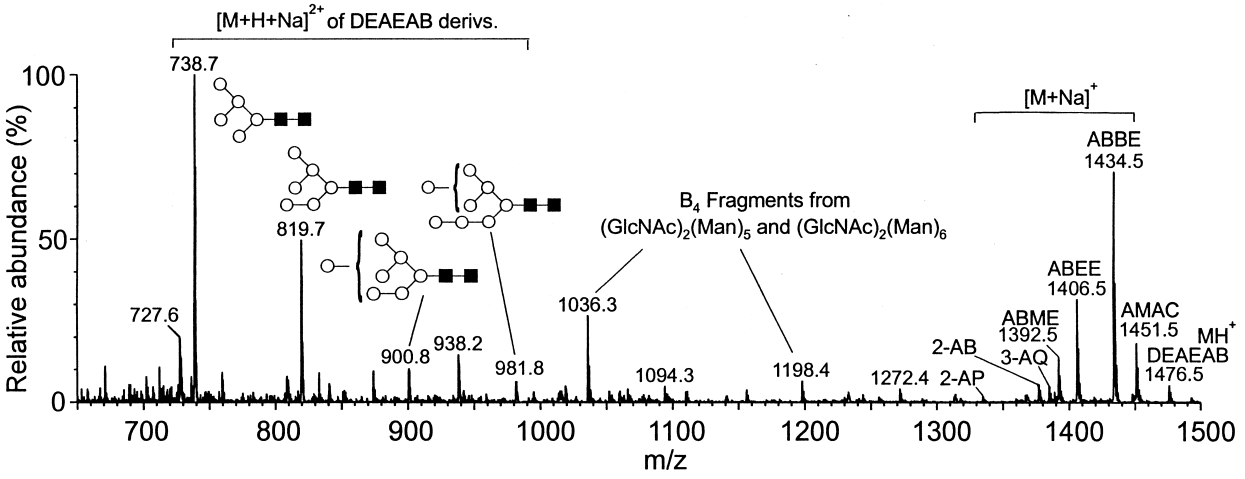

Figure 1. Mass spectrum of equimolar amounts of high-mannose N-linked glycans released from ribonuclease B by hydrazinolysis and derivatized with seven different amines (see text for abbreviations). The spectrum was obtained from about 10 pmol of each derivative at a cone voltage of 180 V. Symbols for the molecular structures are: open circle = mannose; filled circle = GlcNAc.

to which acetic acid (2 μL) had been added. An excess of the amine was added, followed by sodium cyanoborohydride to give a final concentration of this reagent of about 1 molar. The mixture was heated at 65 °C for 2 h, cooled, applied to a strip (100 × 30 mm) of Whatman 3MM chromatography paper (Whatman International, Maidstone, Kent, UK), and allowed to dry. The paper was placed in a chromatography tank containing acetonitrile and the solvent was allowed to rise to the top of the paper. The spot (about 10 mm diameter) at the origin was cut out and the carbohydrate derivatives were eluted with 160 μL of water. Purification was achieved using a C-18 Millipore "ZipTip" (Millipore, Watford, Herts., UK) according to the instructions supplied by the manufacturer.

Schiff bases/glycosylamine. These were prepared by the above method but in the absence of the sodium cyanoborohydride reducing agent.

MALDI Mass Spectrometry

MALDI mass spectra were recorded with a Micromass TofSpec 2E mass spectrometer (Micromass, Wythenshawe, Manchester, UK) from 2,5-DHB. The delay for the time-lag-focusing ion source was 500 ns and the pulse voltage was 3.4 kV. The acceleration voltage was 20 kV and positive ion spectra were recorded in reflectron mode. Spectra from about 30 laser shots were averaged to produce each spectrum and processing was performed with a MassLynx data system. For sample preparation, the glycan solution (0.5 μL containing about 10 pmol of glycan) was applied to the stainless steel target along with the matrix (0.5 μL of a saturated solution of DHB in acetonitrile) and allowed to dry. The sample was then recrystallised from the minimum volume of ethanol [37].

Electrospray Mass Spectrometry

Electrospray MS and MS/MS spectra were recorded with a Micromass Q-TOF mass spectrometer. The carbohydrate derivatives (15 μL containing approximately 3.6 nmol as measured by HPLC) were diluted with either 5 μL of 0.1% formic acid in methanol:water (1:1 by volume) and 5 μL of a solution of an alkali metal iodide [50 nM/μL, dissolved in methanol:water (1:1 by volume)] or with 10 μL of 0.1% formic acid in methanol:water (1:1 by volume) as described below. They were infused using the nanoflow probe at between 50 and 200 nL/min. The needle voltage was 3000 V and the ion source was maintained at 100 °C. Argon at 20 lb/in.^{2} was used as the collision gas and the collision energy and cone voltage were adjusted as described below. The resolution of MS1 was set to unit mass. 60 scans were obtained for each spectrum, with each spectrum being recorded in 1 s (48 spectra/min including interscan delay) and the signal was accumulated until a satisfactory signal/noise ratio had been obtained.

Results

Relative Sensitivities of the Various Derivatives

In order to determine which of the derivatives gave the most intense signals when prepared as described above, saturating concentrations from Millipore ZipTips of $(GlcNAc)_2(Man)_5$ (I), derivatized with each of the amines, were mixed and examined by microflow electrospray from methanol:water (1:1 by volume) containing 100 pmol/μL sodium iodide. $[M + Na]^+$ ions were observed as the major ion from all derivatives except DEAEAB where the $[M + H + Na]^{2+}$ ions dominated the profile (Figure 1). A similar high sensitivity of the doubly charged ion has been observed following elec-

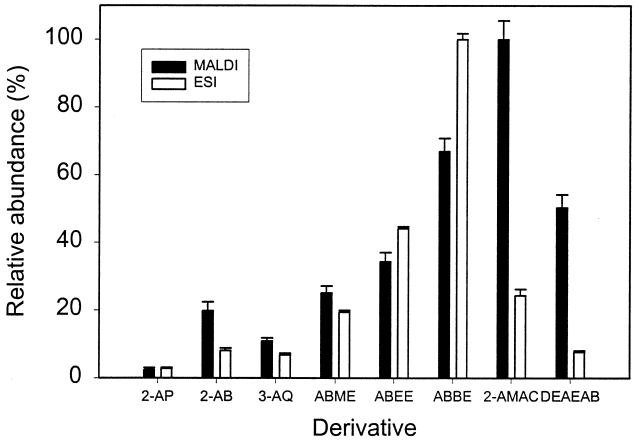

Figure 2. Comparison of the MALDI (solid bars) and electrospray (shaded bars) signal strengths from the high-mannose N-linked glycan $(GlcNAc)_2(Man)_5$ derivatized by reductive amination with each of eight different amines.

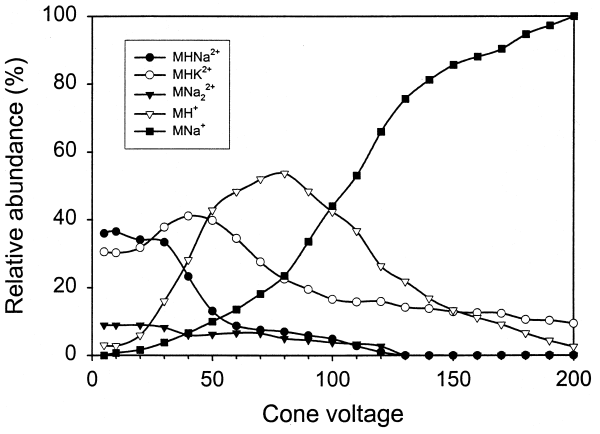

Figure 3. Relative intensities of singly and doubly charged ions from the 2-AB derivative of $(GlcNAc)_2(Man)_5$ recorded at various cone voltages with 0.1% formic acid added to the electrospray solvent. Each point is a measurement of the absolute ion abundance from the average of 11 spectra.

trospray [38] ionization of the analogous ester and has been attributed to the high proton affinity of the tertiary amine. The relative signal strengths of the $[M + Na]^+$ ions from a single glycan derivatized with each of the amines are compared in Figure 2 where it can be seen that the derivative from butyl-4-aminobenzoate provided the highest sensitivity for singly charged ions following electrospray. The signal strength dropped with the chain length (ethyl and methyl esters) of the derivative. A similar relationship has been reported by Poulter and Burlingame [2] using negative ion FAB ionization. Suzuki et al. [10] also report increased sensitivity of the ethyl ester compared with that provided by the 2-AP derivative in methanol:water when observed both as $[M + H]^+$ and $[M - H]^-$ ions. When the above mixture of eight derivatives was examined by MALDI mass spectrometry, the 2-AMAC derivative was found to give the most intense signal (Figure 2). It must be emphasized, however, that these results reflect the overall sensitivity of the experiment. As optimal conditions for derivatization with each amine were not determined, the final signal strength will reflect factors such as product yield and losses during cleanup as well as mass spectrometric ionization efficiency.

Effect of Cone Voltage on Ion Yield

Addition of small amounts (0.1%) of formic acid to the electrospray solvent (methanol:water; 1:1 by volume) induced protonation of the derivatized glycan. Results for the 2-AB derivative of $(GlcNAc)_2(Man)_5$ (I) (Figure 3), which were typical, showed that the $[M + H]^+$ ion was present at maximum intensity at a cone voltage of about 80 V, but only reached about half of the maximum intensity of the $[M + Na]^+$ ion. Various doubly charged ions were formed ($[M + H + Na]^{2+}$, $[M + H + K]^{2+}$, and $[M + 2Na]^{2+}$) but their intensities did not reach those of the maximum reached by the singly charged ions under any conditions. No $[M + 2H]^{2+}$ ions were observed in this experiment. Replacement of the formic acid with sodium acetate or iodide (50 nmol/μL) suppressed protonation and gave only the $[M + Na]^+$ and $[M + 2Na]^{2+}$ ions for all derivatives except that formed from 2-(*NN*-diethylaminoethyl)-4-aminobenzoic acid (DEAEAB). The relative abundance of the $[M + Na]^+$ ion again increased with cone voltage, as before, up to the maximum attainable of 200 V, whereas the abundance of the $[M + 2Na]^{2+}$ ion maximized at a cone voltage of about 60 V but with an abundance of only 20% of the $[M + 2Na]^{2+}$ ion. The absolute abundance of the $[M + Na]^+$ ion, relative to that in the spectra recorded in the presence of formic acid, was only slightly enhanced, suggesting that sufficient residual sodium was present in the latter solvent to ionize most molecules. Similar profiles were obtained for the potassium adducts, for underivatized glycans and for glycans derivatized with amines other than DEAEAB.

MS/MS Fragmentation

The energy needed to fragment compounds under CID conditions increased as a function of the charge state, adduct, and molecular weight of the compound under investigation. Previous results [25] have shown a linear relationship between collision cell voltage and increasing mass for a given charge state and adduct, with about 100 V being needed to fragment the $[M + Na]^+$ ion from a sugar of mass ~2 kDa. $[M + H]^+$ ions require about half of this voltage and multiply charged ions even less. Consequently, the spectra reported in this paper were not recorded under exactly the same conditions. In order to detect minor fragments, the collision cell voltage was varied by approximately 10 V on either side of optimum so that fragments could be collected over the entire mass range. Also, spectra were recorded for several minutes in order to maximize the

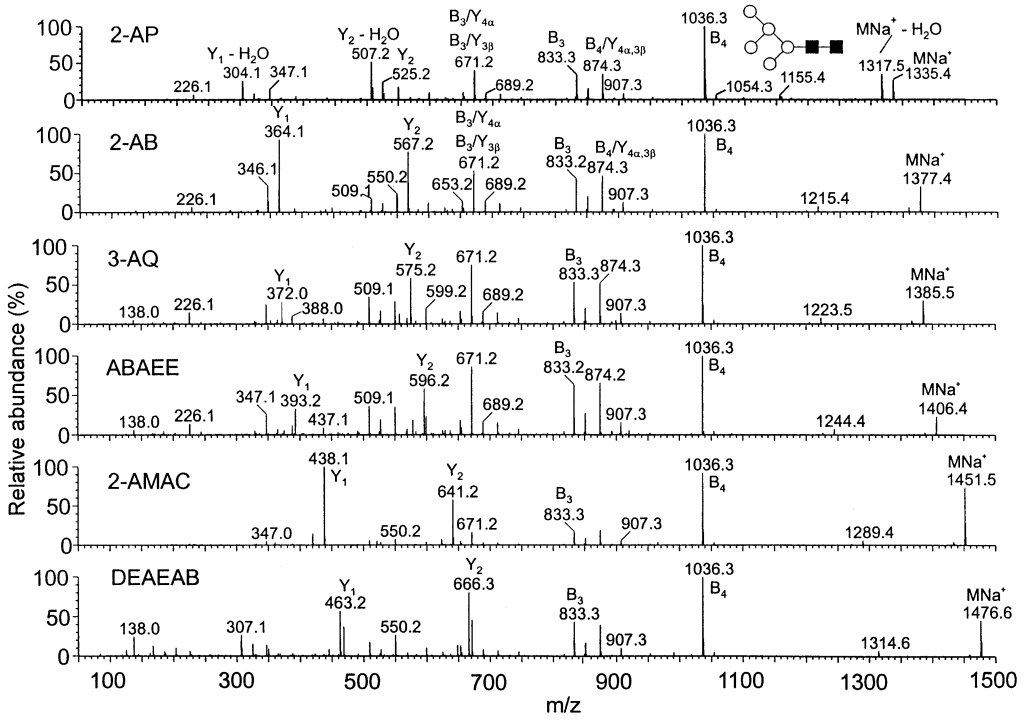

Figure 4. Electrospray CID mass spectra of the $[M + Na]^+$ ions from six derivatives of $(GlcNAc)_2(Man)_5$. (Abbreviations are listed in the Materials and Methods section). Symbols for the structures are as defined in the legend to Figure 1.

signal/noise ratio and record even the minor fragments. Spectra containing all major fragments could be obtained from only about 3 s of recording using the 3-AQ or 2-AB derivatives. The amount of sample consumed during this time was calculated at about 7 pmol based on a saturating concentration of the derivatives extracted by the ZipTip of 3.6 nmol. The DEAEAB derivatives gave an increase in sensitivity of about 100-fold over that of the free glycan.

$[M + Na]^+$ ions. The nature of the derivative was found to have little effect on the appearance of the spectra derived from the $[M + Na]^+$ ions, as shown for six derivatives of $(GlcNAc)_2(Man)_5$ (I, Figure 4), suggesting that the sodium atom was associated with the sugar rather than with the derivative. These spectra were also similar to that from the underivatized glycans [25], the exceptions being those the $^{0,2}A_5$ and $^{2,4}A_5$ ions (Domon and Costello [26] nomenclature) were missing as the result of the opened and reduced reducing-terminal GlcNAc ring. The main difference between the spectra of each of the derivatized sugars was in the mass of the Y_1 and Y_2 ions (Figure 4) as these ions contained the derivatized portion of the molecule. The relative abundance of these two ions was much greater in the spectra of the 2-AMAC derivatives than in the spectra of the other derivatives, thus making it more difficult to observe the minor cross-ring cleavage ions in the spectra of these derivatives. In the spectrum of the 2-AP derivatives, these ions showed a favorable loss of water, as did the molecular ion. The clearest spectra were obtained from the 3-AQ derivatives. It was noted earlier [13] that the diagnostic $^{0,4}A_3$ cross-ring fragment ion (see below) expected in the spectra of the 2-AB derivative of $(GlcNAc)_2(Man)_5$ (I), currently the derivatives of choice in this laboratory for HPLC studies, were coincident in mass with the Y_2 ion. Formation of the 3-AQ derivative enabled these ions to be separated without causing any further loss of diagnostic ions. The relative abundance of cross-ring fragments also appeared to be greater in the spectra of these derivatives than in the spectra of the others.

Detailed fragmentation of the high-mannose glycan $(GlcNAc)_2(Man)_5$ (I). The CID spectrum of the $[M + Na]^+$ adduct of the 3-AQ derivative of $(GlcNAc)_2(Man)_5$ (I) is shown in Figure 5. Although this spectrum was recorded from about 100 pmol (consumed) of glycan, even the minor cross-ring cleavage ions were still visible in spectra recorded from 10 pmol. Most of the major fragment ions were the result of glycosidic cleavages. A prominent B_4 ion was present at *m/z* 1036.4 and this ion fragmented further by successive losses of mannose to give the ions at *m/z* 874.3, 712.3, 550.1, 388.1, and 226.0. Corresponding losses from the molecular ion (*m/z* 1223.5, 1061.4, 899.4, 737.3) were weak but, in both series, the ion representing loss of three mannose residues (e.g., $B_4/Y_{3\alpha}$) was relatively more abundant than the others as the result of loss of the three mannose residues from the 6-antenna by the net breaking of a

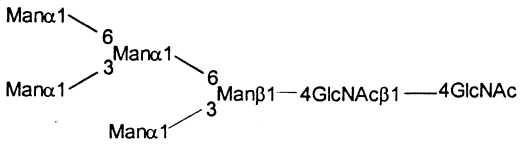

I, High-mannose N-linked glycan $(GlcNAc)_2(Man)_5$

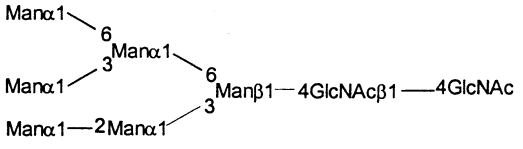

II, High-mannose N-linked glycan $(GlcNAc)_2(Man)_6$

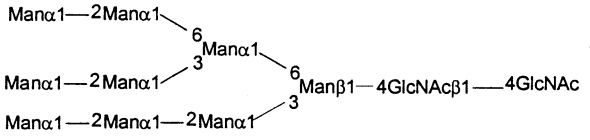

III, High-mannose N-linked glycan $(GlcNAc)_2(Man)_9$

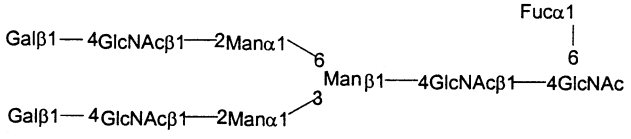

IV, Fucosylated biantennary glycan

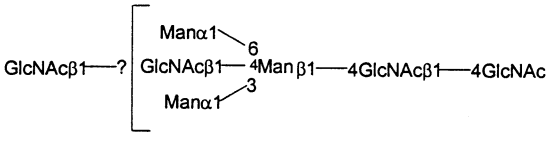

V

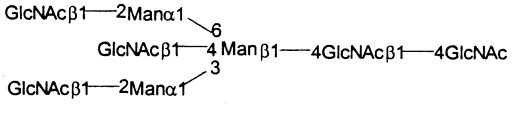

VI

single bond. However, it must be borne in mind that, as all of these glycosidic cleavage reactions involved a hydrogen transfer, usually from a hydroxyl group [32], the relative positions of the abstracted hydrogen and acceptor oxygen atom will also affect the ion yield and the presence of an abundant ion may not necessarily imply the existence of a single cleavage. The abundant loss of three mannose residues seen in the spectrum of

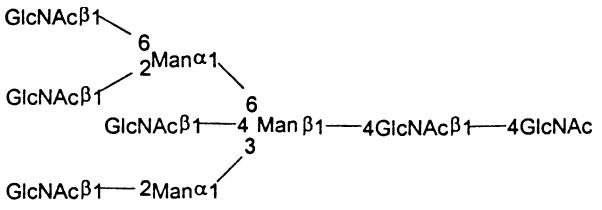

VII

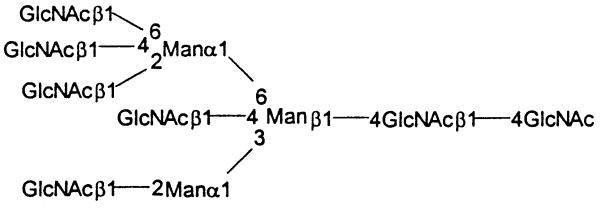

VIII

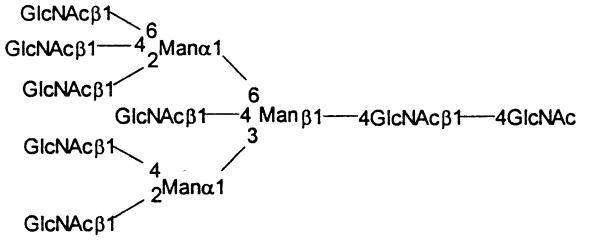

IX

the sodium adduct of $(GlcNAc)_2(Man)_5$ was also seen in the spectrum of $(GlcNAc)_2(Man)_6$ (II) from ribonuclease (data not shown) where the extra mannose residue is known to be on the 3-antenna [39] and is, thus, retained.

As illustrated by the above fragmentations, the majority of ions from these N-linked glycans were "internal fragments" (formed by losses from two or more regions of the molecule) and could have several routes of formation. These internal cleavages resulted in spectra that were difficult to interpret if the structure of the molecule was unknown. However, examination of several spectra allowed some generalizations to be made. Thus, differentiation of high-mannose or hybrid structures from complex (both antenna processed) N-linked sugars could be made by the presence of $(Hex)_xNa^+$ ions where x was greater than three. In the spectrum shown in Figure 5, $(Hex)_xNa^+$ ions occurred at m/z 185.0 ($x = 1$), 347.1 ($x = 2$), 509.1 ($x = 3$), 671.2 ($x = 4$), and 833.3 ($x = 5$, B_3 ion). It would appear that the ion at m/z 671.3 is composed mainly of the B_3 ion minus the mannose residue attached to the 3-position of the branching mannose. Ions formed by this route are generally among the most abundant in spectra obtained by PSD [40] or high energy CID [30] and define the composition of the 6-antenna.

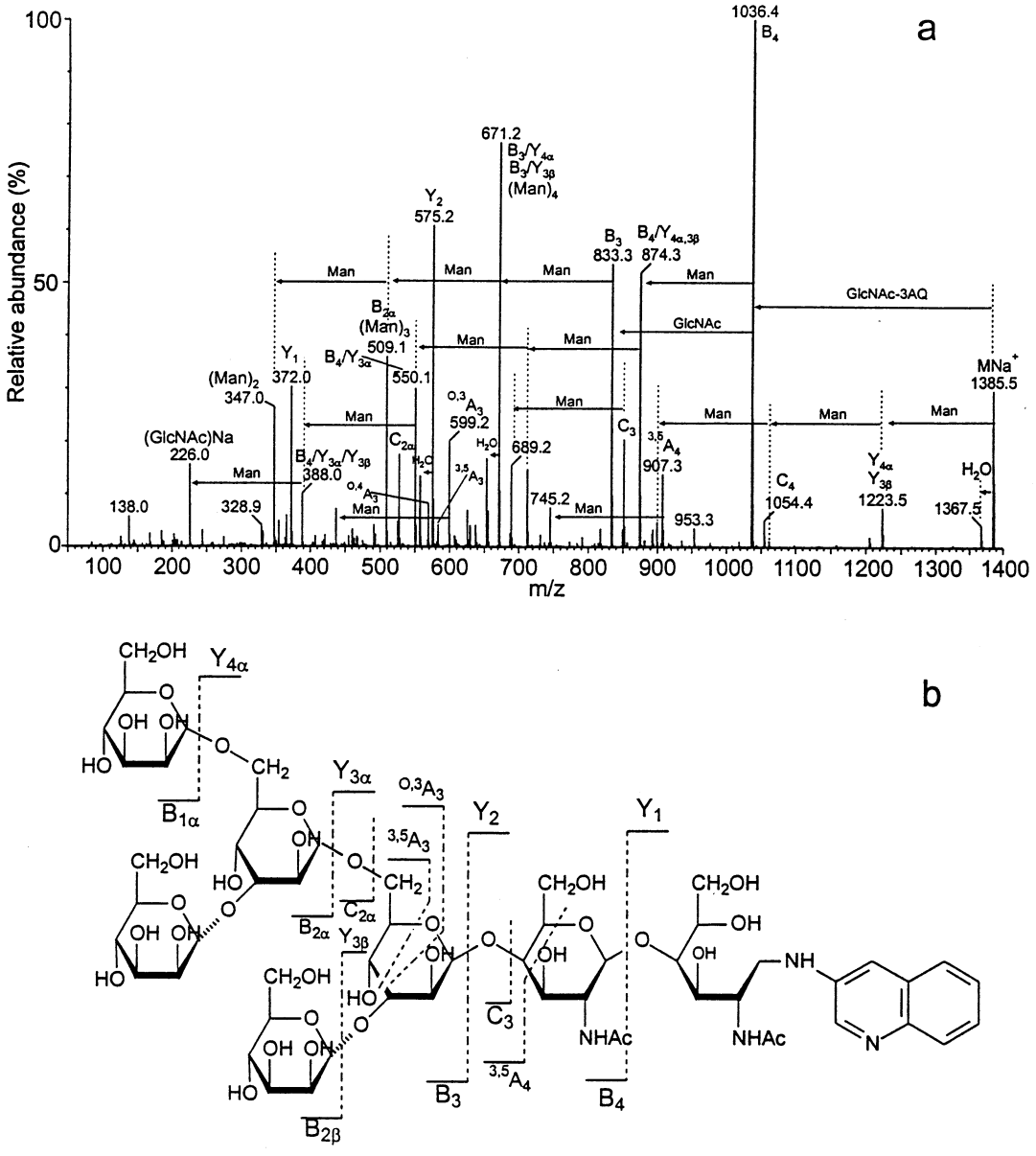

Figure 5. (**a**) Electrospray CID mass spectrum of the $[M + Na]^+$ ion from the 3-AQ derivative of $(GlcNAc)_2(Man)_5$ (approximately 100 pmol consumed). The arrows in this and other figures indicate mass differences and do not necessarily imply a fragmentation path. (**b**) Scheme showing the proposed routes of formation of the various ions shown in (a).

Cross-ring fragments, and internal fragments derived from them, were relatively weak but were present at *m/z* 907.3 ($^{3,5}A_4$), 745.2 [$^{3,5}A_4/Y_4$ (or $Y_{3\beta}$)], 599.2 ($^{0,3}A_3$), 583.2 ($^{3,5}A_3$), and 569.2 ($^{0,4}A_3$). The three A_3 ions were diagnostically useful in that they were formed by bisection of the branching mannose residue and, thus, contained only the monosaccharide residues from the 6-antenna. Five other ions (*m/z* 609.2, 625.2, 629.2, 637.2, and 655.2) also contained the mannose residues attached to the 6- but not to the 3-antennae. Their structures and mechanisms of formation were uncertain, although structures such as those shown in Table 2 can be proposed. The ions at *m/z* 637.2 and 655.2, which differed by the mass of one oxygen atom, appeared to contain the intact core mannose ring but not the substituents attached to C-1 and C-3 or their linking oxygen atoms. The other three ions appeared to be cross-ring cleavage products that had lost the substituent at C-3. The abundant cross-ring cleavage ions from the reducing-terminal GlcNAc residue that were seen in the spectra of the underivatized glycans [30, 40] were either absent, or very weak, in the spectra of these derivatized compounds. X-type fragments were absent, even though they were major fragments in spectra recorded at high energy [30].

MS^3 experiments were performed on several of the

Table 2. Proposed structures of the ions formed by cleavages across and around the core mannose residue of $(GlcNAc)_2(Man)_5$. All structures were in the form of $[M + Na]^+$ ions

m/z	Structures
569.2	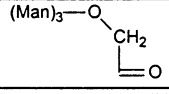
588.2	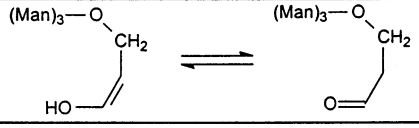
599.2	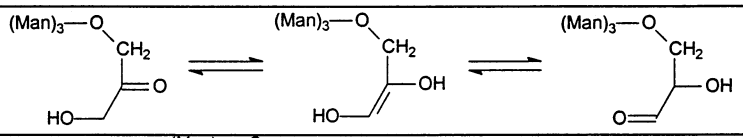
609.2	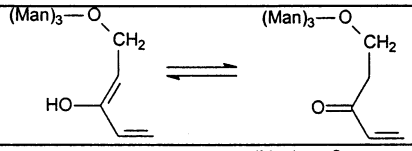
625.2	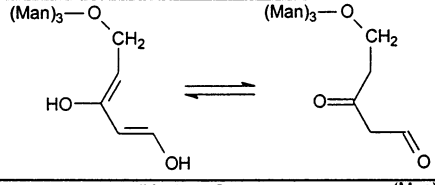
629.2	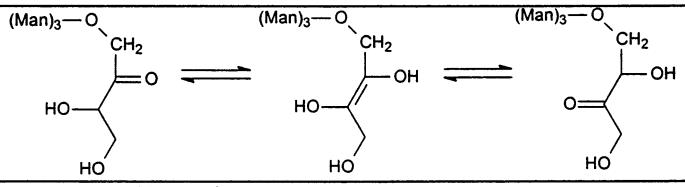
637.2	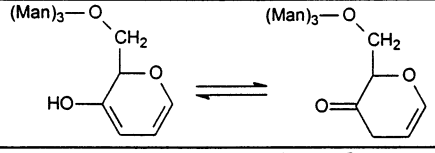
655.2	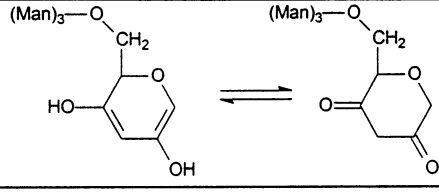

abundant fragments from the $[M + Na]^+$ ion of $(GlcNAc)_2(Man)_5$-3-AQ by using cone-voltage fragmentation to produce the second-generation ions. Two of the spectra are shown in Figure 6. The B_3 [$(Man)_5$, *m/z* 833.3], $[B_3 - Man]^+$ [$(Man)_4$, *m/z* 671.2], and $[B_3 - (Man)_2]^+$ [$(Man)_3$, *m/z* 509.1] ions gave simple spectra showing mainly successive losses of mannose. The B_4 (*m/z* 1036.3) and $[B_4 - Man]^+$ (*m/z* 874.3) ions fragmented to give spectra similar to that given by the molecular ion with the exception that the Y_1 and Y_2 ions were missing. Cross-ring cleavage fragments, e.g., $^{3,5}A_4$, $^{3,5}A_3$, $^{0,4}A_3$, $^{0,3}A_3$, and ($^{0,3}A_3$ − Man) were relatively more abundant in these spectra than in the spectra of the parent compound. These spectra confirmed that the internal cleavage fragments could be formed by several competing pathways.

Detailed fragmentation of the high-mannose glycan $(GlcNAc)_2(Man)_9$ (III). The mass spectrum of the $[M + Na]^+$ ion from the 3-AQ derivative of $(GlcNAc)_2(Man)_9$ is shown in Figure 7. The spectrum showed the same general features as that of the corresponding derivative of $(GlcNAc)_2(Man)_5$. Glycosidic cleavages resulting in successive losses of mannose residues dominated the spectrum. The branching pattern was reflected in the relative abundances of the internal cleavages resulting from mannose losses from the B_4 and B_5 ions. These ions were most abundant when the mannose loss involved a single cleavage. Thus, loss of two, three, and five mannose residues gave the abundant ions at *m/z* 1360.4 (B_5/Y_4), 1198.4 ($B_5/Y_{3\beta}$), and 874.4 ($B_5/Y_{3\alpha}$) from the B_5 ion and *m/z* 1157.4 (B_4/Y_4), 995.4 ($B_4/Y_{3\beta}$), and 671.3 ($B_4/Y_{3\alpha}$) from the B_4 ion, respectively. Cross-ring

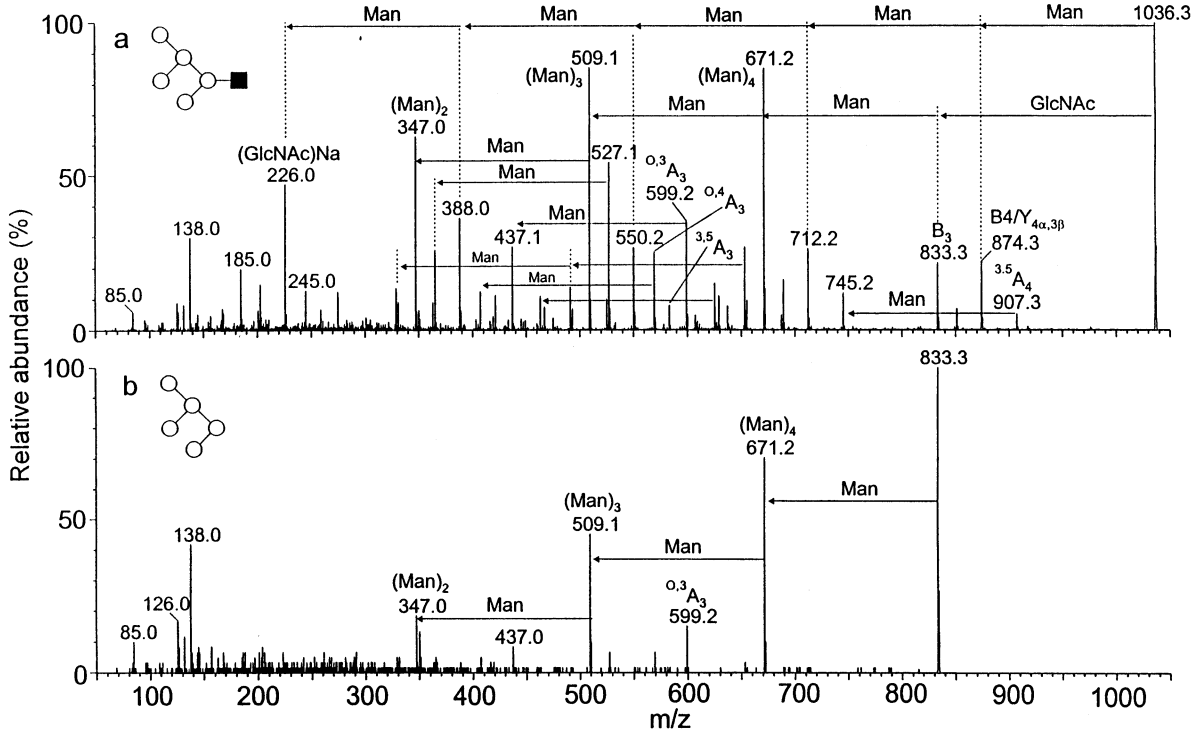

Figure 6. (**a**) MS^3 spectrum of the B_4 ion from $[(GlcNAc)_2(Man)_5\text{-}3AQ + Na]^+$. (**b**) MS^3 spectrum of the B_3 ion from $[(GlcNAc)_2(Man)_5\text{-}3AQ + Na]^+$.

fragments were relatively abundant and were observed from the two GlcNAc residues and from the two branching mannose residues as shown in Figure 7. These ions defined the branching pattern at the two branch points. Most of these cross-ring fragments were observed to lose additional mannose residues.

Detailed fragmentation of the biantennary complex glycan $(Gal)_2(GlcNAc)_4(Man)_3(Fuc)_1$-3AQ (IV). The spectrum of the $[M + Na]^+$ ion from the 3-AQ derivative of the fucosylated biantennary glycan (IV) is shown in Figure 8. Most of the fragment ions were common to the spectrum of the underivatized glycan with major ions being the products of glycosidic cleavages adjacent to GlcNAc residues. Thus, major primary cleavage ions were produced by cleavage of the chitobiose core (B_5, *m/z* 1442.5) and antennae (B_2, *m/z* 388.1, Y_4, *m/z* 1572.6). Prominent internal ions also involved these cleavages to give ions such as *m/z* 1207.4 (Y_4/Y_4) and 1077.4 (B_5/Y_4). Losses of fucose were observed from the molecular ion (to give *m/z* 1791.7) and from the Y ions, e.g., *m/z* 1629.7, 1426.5, 1061.3, 575.2, and 372.1. Many relatively weak A-type (but not X-type) cross-ring fragments were present. Their weakness, compared to that in the spectra of the high-mannose glycans, is probably due to competition with the very favorable glycosidic cleavages resulting in loss of the Gal–GlcNAc residues from the antennae.

Detailed fragmentation of the complex glycans from chicken egg glycoproteins. In addition to the major constituent, ovalbumin, chicken egg white contains a number of other glycoproteins such as ovomucoid and riboflavin binding protein. Both of these compounds have been found as contaminants of commercial ovalbumin and contribute most of the higher molecular weight N-linked sugars present in the glycan mixture [41]. Like many other avian glycans, most of these compounds carry truncated antennae, terminating in GlcNAc. Figure 9 shows the MS/MS spectra of the 2-AB derivatives of five of these compounds of composition $(GlcNAc)_{4-8}(Man)_3$ (V–IX). Although the glycan of composition $(GlcNAc)_8(Man)_3$ (IX, Figure 9e) appears to be a single compound, the others are mixtures of at least two isomers [42–44]. The major isomer of each composition is shown in Figure 9. All of these spectra were dominated by ions produced by successive losses of GlcNAc residues from various precursor ions. The $[M + Na]^+$ ion initiated one series but this series terminated after loss of only three residues. The major series originated from the B_4 ions (loss of GlcNAc-2-AB) and terminated in the ion at *m/z* 712.3 $\{[(GlcNAc)_1(Man)_3 + Na]^+\}$. As noted earlier [30], the glycosidic ion that was most diagnostic of antenna composition can be formally attributed to loss of the intact 3-antenna from the B_3 ion. This ion, although weak, initiated another cascade of GlcNAc losses and was observed at *m/z* 1159.4 in the

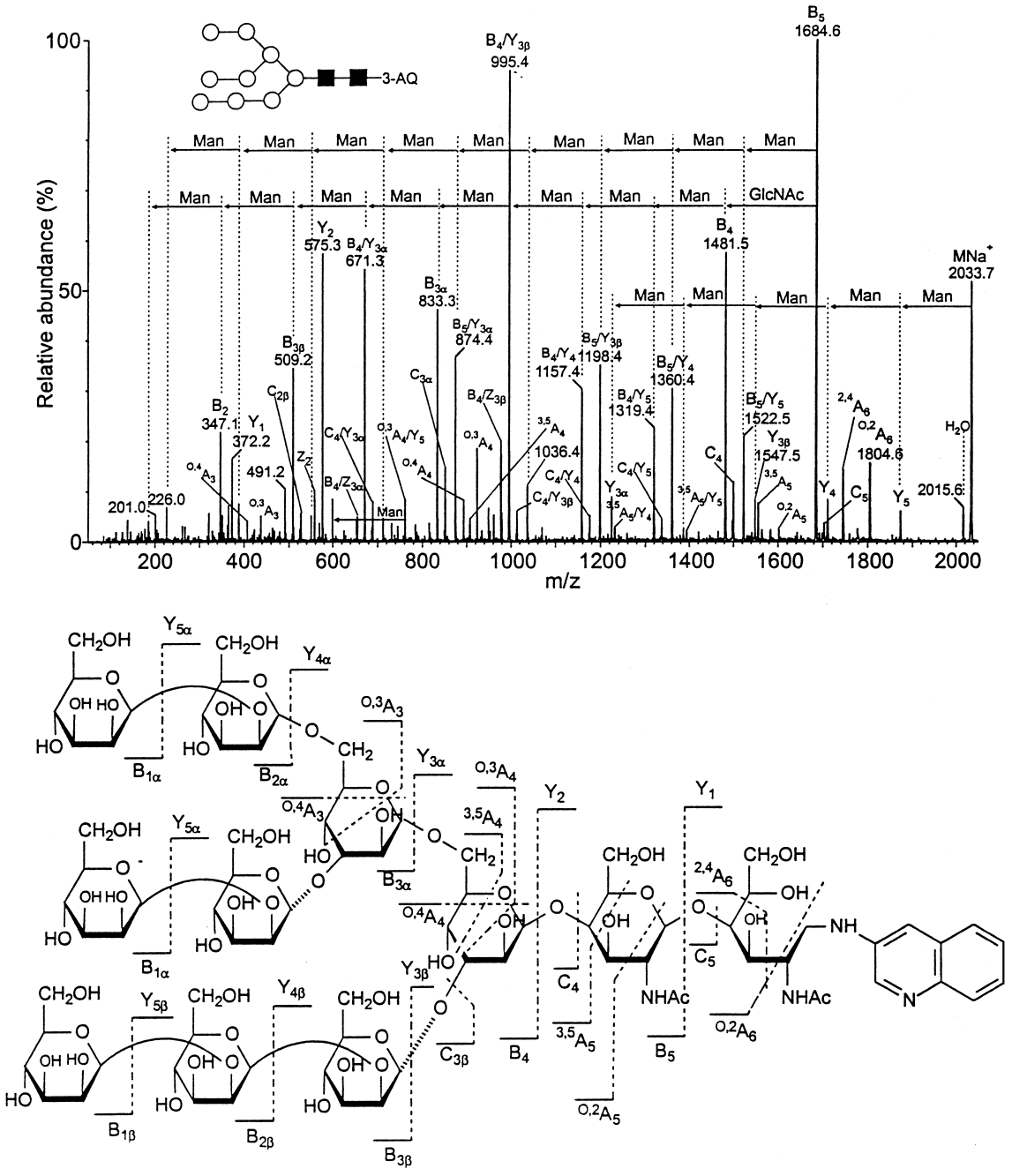

Figure 7. (Top) Electrospray CID mass spectrum from $[(GlcNAc)_2(Man)_9\text{-}3AQ + Na]^+$. Symbols are as defined in the legend to Figure 1. (Bottom) Scheme showing the proposed routes of formation of the various ions shown in (a).

spectra of $(GlcNAc)_8(Man)_3$ (IX) and $(GlcNAc)_7(Man)_3$ (VIII) (Figure 9e, d, respectively), *m/z* 956.3 in the spectrum of $(GlcNAc)_6(Man)_3$ (VII, Figure 9c), and at *m/z* 753.3 in the spectrum of $(GlcNAc)_5(Man)_3$ (VI, Figure 9b). Its appearance at the latter mass in the spectrum of $(GlcNAc)_4(Man)_3$ (V, Figure 9a) suggested that the 6- rather than the 3-antenna is substituted with GlcNAc. Cross-ring cleavage fragments were very weak in the spectra of these compounds as the result of the very favorable loss of several GlcNAc moieties.

$[M + H]^+$ ions. The spectrum of the $[M + H]^+$ ion [illustrated for the 3-AQ derivative of $(GlcNAc)_2(Man)_5$, Figure 10] was less complex than that of the $[M + Na]^+$ ion. The Y_1 and Y_2 ions were prominent but the remainder of the spectrum was dominated by only two other series of ions: a B_4 ion that lost successive mannose residues and a series of ions resulting from mannose losses from the molecular ion. Ions involving the $Y_{3\alpha}$ cleavage (*m/z* 528.2 and 877.4, loss of the three mannose residues from the 6-antenna) were relatively more

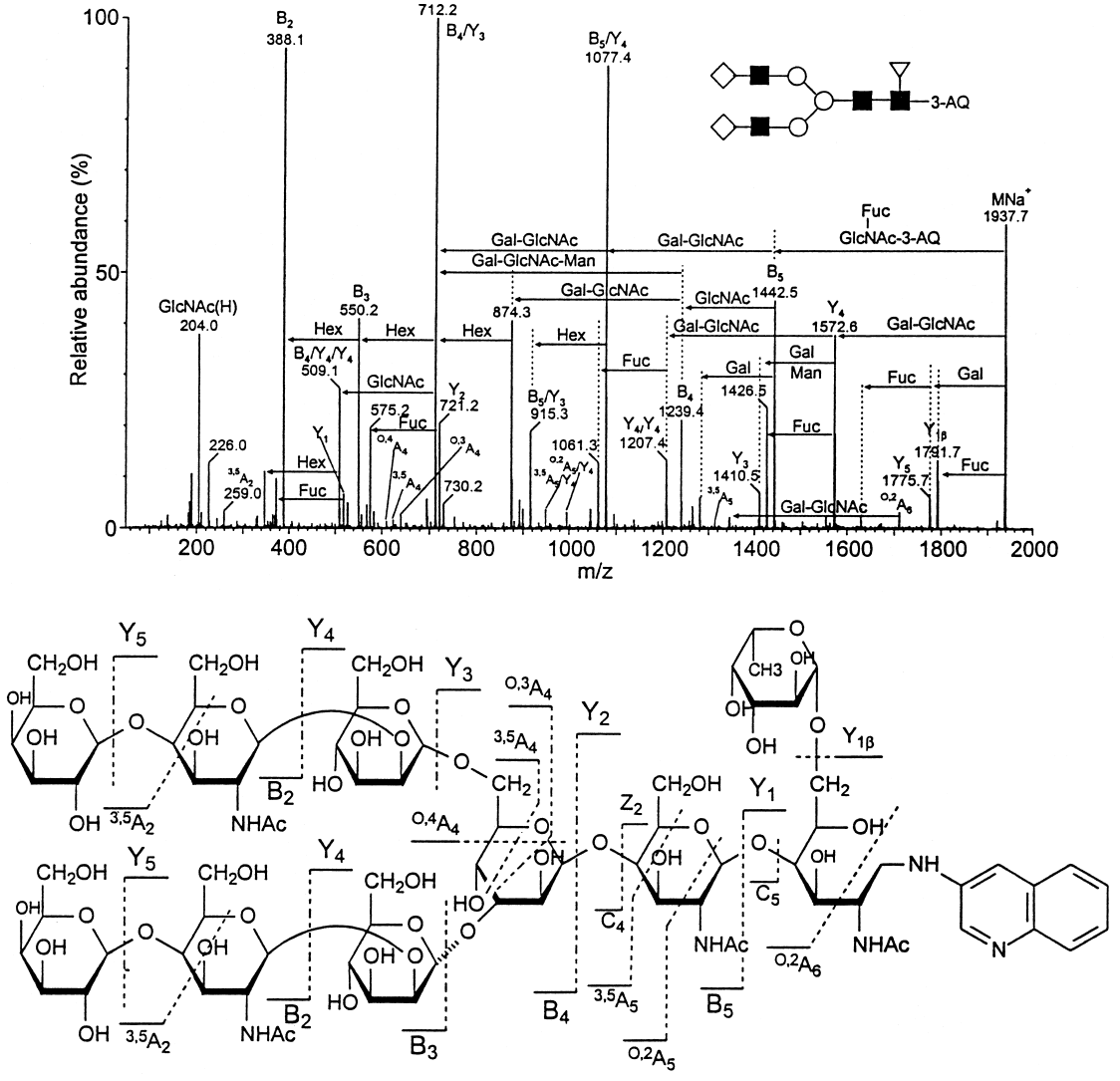

Figure 8. (Top) Electrospray CID mass spectrum of the $[M + Na]^+$ ion from the complex N-linked glycan $[(Gal)_2(GlcNAc)_4(Man)_3(Fuc)_1\text{-}3AQ + Na]^+$. Symbols are as defined in the legend to Figure 1 plus open diamond = galactose, open upside down triangle = fucose. (Bottom) Scheme showing the proposed routes of formation of the various ions shown in (a).

abundant than the other ions of their respective types reflecting the branching pattern. Cross-ring cleavage fragments were absent.

Doubly charged ions. Three doubly charged ions were produced from most derivatives: $[M + 2H]^{2+}$, $[M + H + X]^{2+}$, and $[M + 2X]^{2+}$ where X = the metal adduct. Figure 11 shows the spectra of these ions from the 3-AQ derivative of $(GlcNAc)_2(Man)_5$. The $[M + 2H]^{2+}$ ion (Figure 11a) fragmented mainly by losses of mannose residues to give further doubly charged ions. Losses of mannose, together with a proton, gave weak singly charged ions. Fragmentation of the $[M + H + Na]^{2+}$ ion (Figure 11b) was directed by the proton to give a spectrum that was similar to that from the $[M + 2H]^{2+}$ ion but with a higher proportion of singly charged ions. The Y_1 cleavage ion was observed with both hydrogen and sodium as the adduct. Very little fragmentation was observed from the $[M + 2Na]^{2+}$ ion (Figure 11c).

The effect of other cations on the fragmentation of the $[M + H + X]^{2+}$ ion was also investigated and the results are shown in Figure 12 for the 3-AQ derivative of the high-mannose glycan $(GlcNAc)_2(Man)_6$ (II). There was little difference between the fragment ions produced from the lithium and sodium adducts. The potassium, rubidium, and cesium adducts, however, showed reduced fragmentation, the extent of which decreased as the atomic weight of the adduct increased. Similar observations have been made with fragmentation of these adducts following MALDI ionization [45] and with electrospray MS/MS fragmentation of the free glycan and its DEAEAB derivative [46]. The nature of the fragmentation shown by these larger cation adducts was also different in that major singly charged ions were formed by loss of the metal. Ions corresponding to

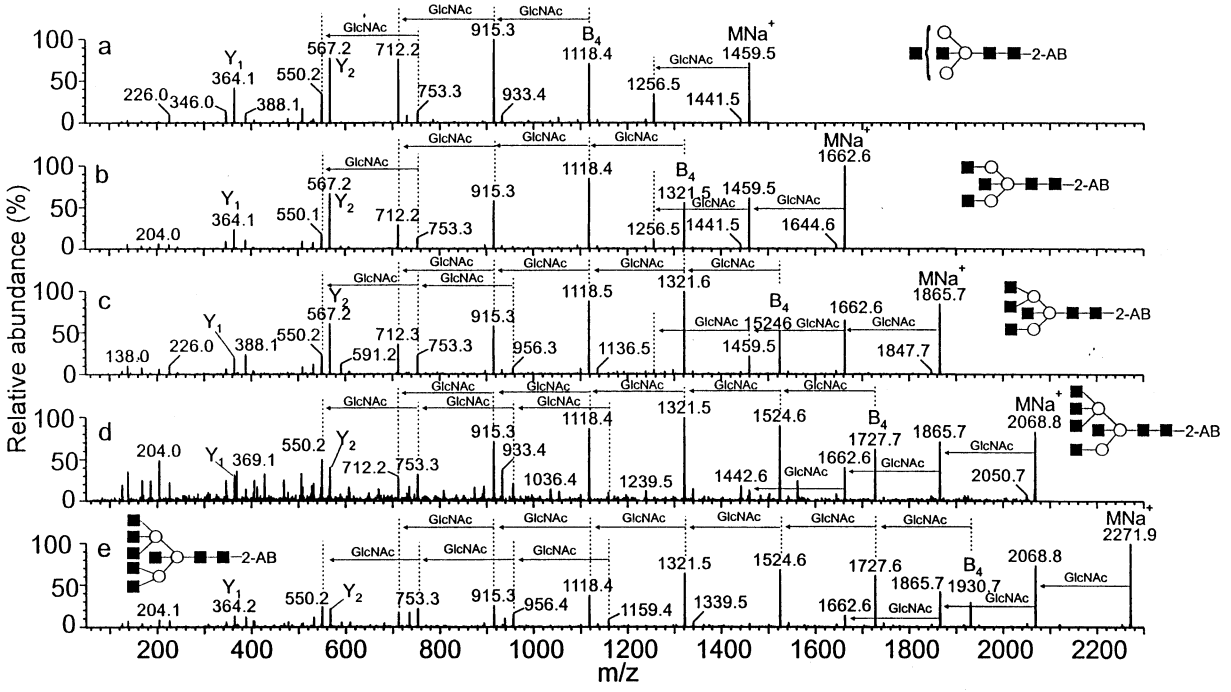

Figure 9. Electrospray CID mass spectrum of the $[M + Na]^+$ ions from the 2-AB derivatives of complex N-linked glycans of composition $(GlcNAc)_{4-8}(Man)_3$ from chicken egg white glycoproteins. Symbols are as defined in the legend to Figure 6.

the metal itself were also observed [47]. The singly charged $[M + H]^+$ ions, resulting from metal ion loss from the potassium and rubidium adducts, gave a series of singly charged ions resulting from successive losses of mannose residues.

Schiff Base/Glycosylamine Derivatives

These derivatives were prepared by omitting the sodium cyanoborohydride reducing agent from the above (reductive amination) method in order to check their

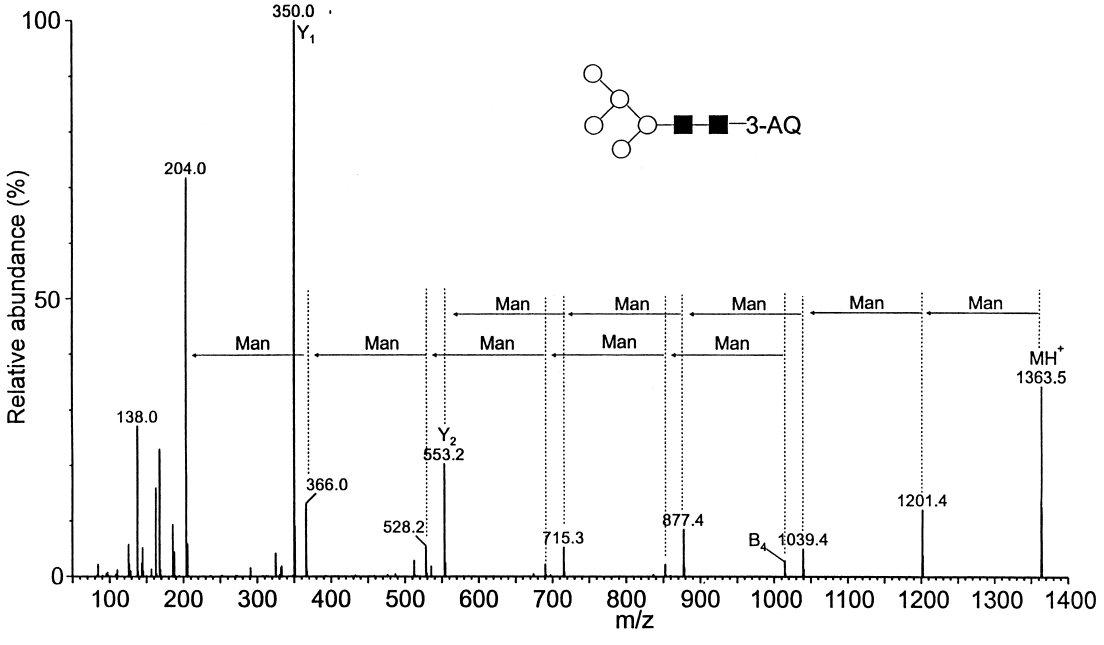

Figure 10. Electrospray CID mass spectrum of the $[M + H]^+$ ion from the 3-AQ derivative of $(GlcNAc)_2(Man)_5$. The collision cell voltage was 40 V.

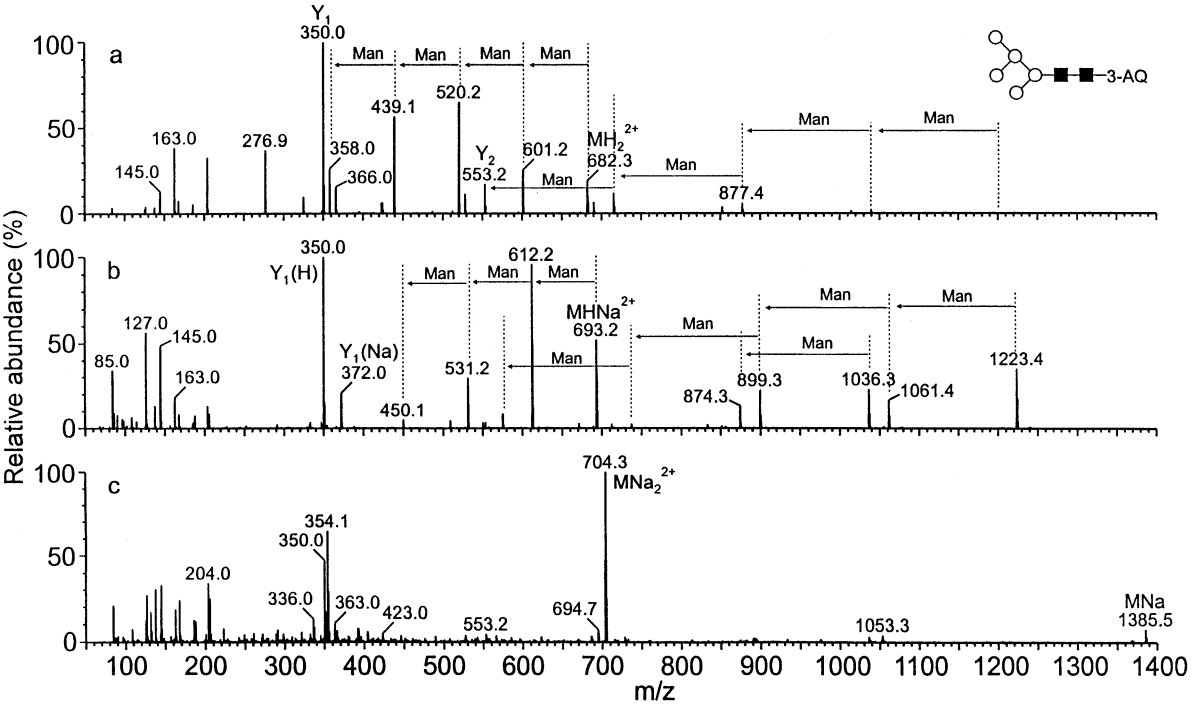

Figure 11. Electrospray CID mass spectra of the $[M + 2H]^{2+}$ (**a**), $[M + H + Na]^{2+}$ (**b**), and $[M + 2Na]^{2+}$ (**c**) ions from the 3-AQ derivative of $(GlcNAc)_2(Man)_5$. The collision cell voltage was in the range 20–30 V.

stability and fragmentation properties, as the absence of this reagent would greatly aid the cleanup stage of the derivative preparation. However, as anticipated, these derivatives were relatively unstable and yields were low.

The MS/MS spectra of their $[M + Na]^+$ ions were

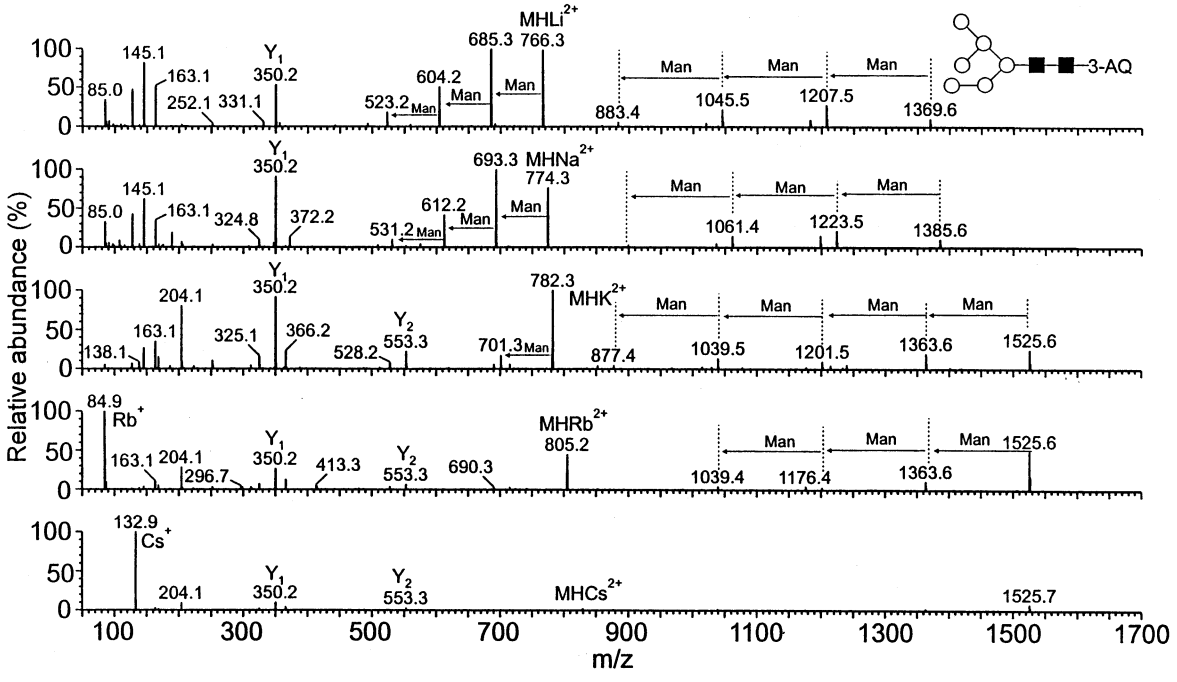

Figure 12. Electrospray CID mass spectra of, from top to bottom, the $[M + H + Li]^{2+}$, $[M + H + Na]^{2+}$, $[M + H + K]^{2+}$, $[M + H + Rb]^{2+}$, and $[M + H + Cs]^{2+}$ ions from the 3-AQ derivative of $(GlcNAc)_2(Man)_6$ (II).

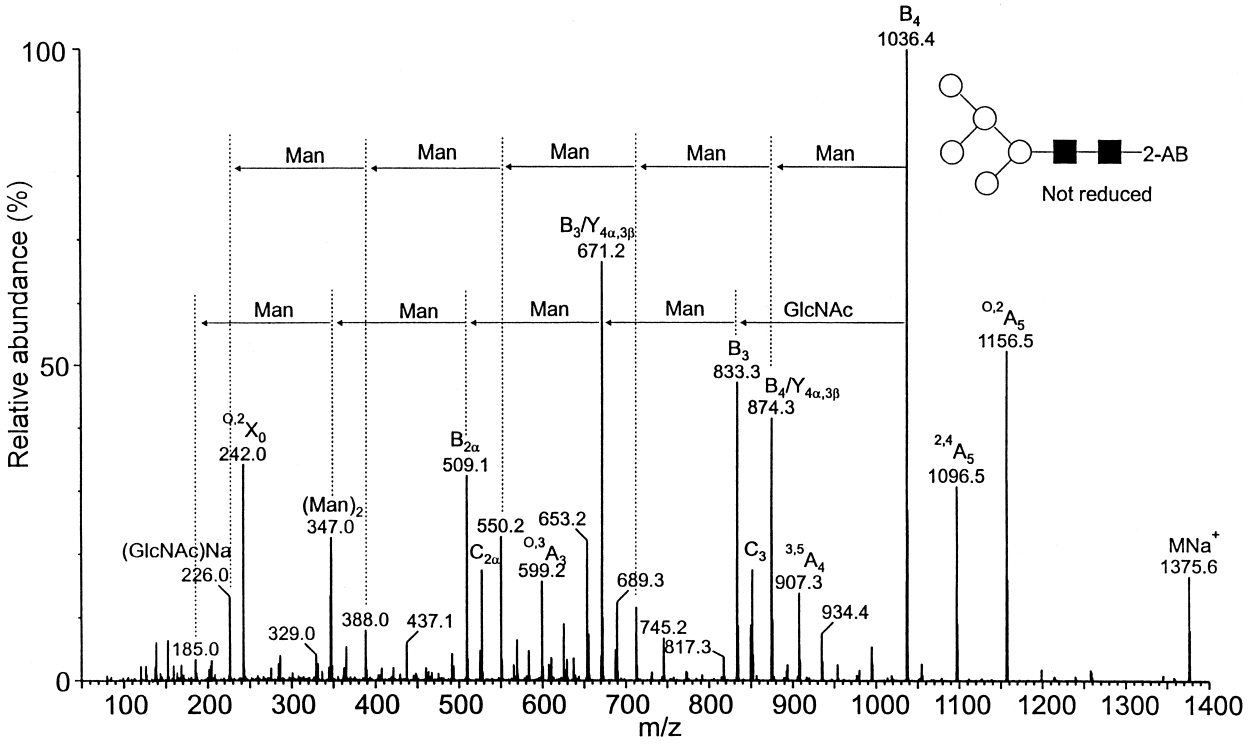

Figure 13. Electrospray CID mass spectra of the $[M + Na]^+$ ion from the 2-AB derivative of $(GlcNAc)_2(Man)_5$ prepared without reduction.

very similar to those of the corresponding reduced derivatives as illustrated for the 2-AB derivative of $(GlcNAc)_2(Man)_5$ (Figure 13). The main differences were the relatively high abundance of the $^{0,2}A_5$ and $^{2,4}A_5$ cross-ring cleavage ions from the reducing-terminal GlcNAc moiety, the low abundance of the Y_1 and Y_2 ions (*m/z* 364.1 and 567.2) and the appearance of the $^{0,2}X_0$ ion at *m/z* 242.0 [CH_3–CO–NH–^{2}CH=^{1}CH–NH–($PhCONH_2$)]. The spectra of the various derivatives of any one particular glycan were very similar except for minor differences of the type shown for the derivatives prepared by reductive amination shown in Figure 4. It is not clear if these derivatives are in the form of the Schiff base or glycosylamine. Spectra of the $[M + H]^+$ and doubly charged ions generally paralleled those of the reduced derivatives with the exception that the $^{0,2}X_0$ ion tended to dominate the fragments the $[M + 2Na]^{2+}$ ions.

Discussion

This study has shown that, whereas the type of reducing-terminal derivative affected the extent and nature of ion formation, it had little effect on the fragmentation pattern, as most fragment ions did not contain the derivatized reducing-terminal GlcNAc residue. For all of the derivatives, except those formed from DEAEAB, the $[M + Na]^+$ ion was invariably the most abundant, even in the absence of added sodium salts. Its fragmentation was similar to that of the underivatized glycan and provided more structural information than the $[M + H]^+$ or the doubly charged ions. Ions containing a hydrogen adduct tended to produce only glycosidic cleavage fragments and not the cross-ring fragments that provided linkage information. Potassium, rubidium, and cesium-containing ions produced less fragmentation. The $[M + Na]^+$ ions produced a wealth of glycosidic and cross-ring fragments that provided considerable information on the structure of the glycans.

Unfortunately, the high cone voltage used to maximize the abundance of these $[M + Na]^+$ ions also produced some cone-voltage fragments which complicated the MS (but not the MS/MS) spectra. In addition, the relative abundance of the $[M + H]^+$, and other molecular ions, fell as a function of increasing mass. Profiling of a glycan mixture was, therefore, not as satisfactory as with a MALDI instrument where few in-source fragment ions are seen and no significant fall in signal intensity with mass appears to occur over the mass range covered by the common N-linked glycans [48]. One solution to these problems would be to record a spectrum of a mixture of glycans using MALDI in order to obtain the glycan profile and then to focus only on the molecular species, revealed by this technique, when the sample is examined further with the Q-TOF instrument. For glycans such as $(GlcNAc)_2(Man)_5$ and the biantennary glycan IV, all major fragments could be recorded from 5 to 10 pmol of glycan consumed. Accumulation of more spectra gave informative linkage-revealing cross-ring fragments, particularly at the

site of a branching mannose residue. These ions were most abundant in the spectra of glycans containing few GlcNAc residues because of the tendency for competing glycosidic cleavages to be particularly favorable adjacent to these residues.

Of the eight derivatives studied, the 2-AMAC derivatives gave the least satisfactory spectra as these compounds produced very abundant Y_1 and Y_2 ions, effectively suppressing the relative abundance of the other ions. However, these derivatives gave the most intense MALDI signals. With the exception of the DEAEAB derivatives which gave doubly charged ions as the major species, there was little to choose between the others with respect to fragmentation patterns. One point that was noted, however, was the tendency of the Y_1 and Y_2 ions from the 2-AB derivatives to be coincident in mass with two of the diagnostic cross-ring cleavage ions from $(GlcNAc)_2(Man)_5$ [13]. By varying the mass of the derivative, this problem could be overcome. The best derivative in this respect was that formed from 3-AQ. In addition, this derivative appeared to produce the most abundant fragment ions.

Sialylated glycans could not be cleaned up with C-18 ZipTips in the same way as the neutral compounds. However, in most cases, samples of these compounds were found to give strong positive ion signals without clean-up on C-18 but with several ions from each compound as the result of sodium salt formation. Spectra of the sialylated glycans were also obtained following preparation of their methyl esters [49], a procedure which neutralized the carboxylic acid function and prevented salt formation, thus giving only one ion from each compound. Positive ion fragmentation spectra were dominated by ions resulting from loss of sialic acid but, in other respects, showed the same general features as the spectra of the neutral glycans. Further information is given in the paper specifically describing the fragmentation of the DEAEAB derivatives [46].

Acknowledgments

I thank Professor R. A. Dwek Director of the Glycobiology Institute for his help and encouragement. Thanks are also due to Louise Royle for measuring the concentration of derivatized glycans adsorbed onto C-18 ZipTips. This work was supported by grants from the Biotechnology and Biological Sciences Research Council.

References

1. Hase, S. Precolumn derivatization for chromatographic and electrophoretic analysis of carbohydrates. *J. Chromatogr. A* **1996,** *720*, 173–182.
2. Poulter, L.; Burlingame, A. L. Desorption mass spectrometry of oligosaccharides coupled with hydrophobic chromophores. *Methods Enzymol.* **1990,** *193*, 661–689.
3. Takao, T.; Tambara, Y.; Nakamura, A.; Yoshino, K.-I.; Fukuda, H.; Fukuda, M.; Shimonishi, Y. Sensitive analysis of oligosaccharides derivatised with 4-aminobenzoic acid 2-(diethylamino)ethyl ester by matrix-assisted laser desorption/ionization mass spectrometry. *Rapid Commun. Mass. Spectrom.* **1996,** *10*, 637–640.
4. Hase, S.; Ibuki, T.; Ikenaka, T. Reexamination of the pyridylamination used for fluorescence labelling of oligosaccharides and its application to glycoproteins. *J. Biochem. (Tokyo)* **1984,** *95*, 197–203.
5. Tokugawa, K.; Oguri, S.; Takeuchi, M. Large scale preparation of PA-oligosaccharides from glycoproteins using an improved extraction method. *Glycoconjugate J.* **1996,** *13*, 53–56.
6. Suzuki-Sawada, J.; Umeda, Y.; Kondo, A.; Kato, I. Analysis of oligosaccharides by on-line high-performance liquid chromatography and ion-spray mass spectrometry. *Anal. Biochem.* **1992,** *207*, 203–207.
7. Gu, J.; Hiraga, T.; Wada, Y. Electrospray ionization mass spectrometry of pyridylaminated oligosaccharide derivatives: sensitivity and in-source fragmentation. *Biol. Mass Spectrom.* **1994,** *23*, 212–217.
8. Okamoto, M.; Takahashi, K.; Doi, T.; Takimoto, Y. High-sensitivity detection and postsource decay of 2-aminopyridine-derivatized oligosaccharides with matrix-assisted laser desorption-ionization mass spectrometry. *Anal. Chem.* **1997,** *69*, 2919–2926.
9. Okamoto, M.; Takahashi, K.-I.; Doi, T. Sensitive detection and structural characterization of trimethyl(p-aminophenyl)-ammonium-derivatized oligosaccharides by electrospray ionization-mass spectrometry and tandem mass spectrometry. *Rapid Commun. Mass Spectrom.* **1995,** *9*, 641–643.
10. Suzuki, S.; Kakehi, K.; Honda, S. Comparison of the sensitivities of various derivatives of oligosaccharides in LC/MS with fast atom bombardment and electrospray ionization interfaces. *Anal. Chem.* **1996,** *68*, 2073–2083.
11. Bigge, J. C.; Patel, T. P.; Bruce, J. A.; Goulding, P. N.; Charles, S. M.; Parekh, R. B. Nonselective and efficient fluorescent labeling of glycans using 2-aminobenzamide and anthranilic acid. *Anal. Biochem.* **1995,** *230*, 229–238.
12. Anumula, K. R.; Dhume, S. T. High resolution and high sensitivity methods for oligosaccharide mapping and characterization by normal phase high performance liquid chromatography following derivatization with highly fluorescent anthranilic acid. *Glycobiology* **1998,** *8*, 685–694.
13. Harvey, D. J. Collision-induced fragmentation of 2-aminobenzamide-labelled neutral N-linked glycans. *The Analyst* **2000,** *125*, 609–617.
14. Okafo, G.; Burrow, L.; Carr, S. A.; Roberts, G. D.; Johnson, W.; Camilleri, P. A coordinated high-performance liquid chromatographic, capillary electrophoretic, and mass spectrometric approach for the analysis of oligosaccharide mixtures with 2-aminoacridone. *Anal. Chem.* **1996,** *68*, 4424–2230.
15. Okafo, G.; Langridge, J.; North, S.; Organ, A.; West, A.; Morris, M.; Camilleri, P. High-performance liquid chromatographic analysis of complex N-linked glycans derivatized with 2-aminoacridone. *Anal. Chem.* **1997,** *69*, 4985–4993.
16. Camilleri, P.; Tolson, D.; Birrell, H. Direct structural analysis of 2-aminoacridone derivatised oligosaccharides by high-performance liquid chromatography/mass spectrometric detection. *Rapid Commun. Mass Spectrom.* **1998,** *12*, 144–148.
17. North, S.; Birrell, H.; Camilleri, P. Positive and negative ion matrix-assisted laser desorption/ionization time-of-flight mass spectrometric analysis of complex glycans released from hen ovalbumin and derivatized with 2-aminoacridone. *Rapid Commun. Mass Spectrom.* **1998,** *12*, 349–356.
18. Charlwood, J.; Langridge, J.; Tolson, D.; Birrell, H.; Camilleri, P. Profiling of 2-aminoacridone derivatised glycans by electrospray ionization mass spectrometry. *Rapid Commun. Mass Spectrom.* **1999,** *13*, 107–112.
19. Charlwood, J.; Langridge, J.; Camilleri, P. Structural characterisation of N-linked glycan mixtures by precursor ion scan-

ning and tandem mass spectrometric analysis. *Rapid Commun. Mass Spectrom.* **1999,** •••, 1522–1530.
20. Charlwood, J.; Birrell, H.; Camilleri, P. Carbohydrate release from picomole quantities of glycoprotein and characterisation of glycans by high-performance liquid chromatography and mass spectrometry. *J. Chromatogr. B* **1999,** *734*, 169–174.
21. Charlwood, J.; Birrell, H.; Bouvier, E. S. P.; Langridge, J.; Camilleri, P. Analysis of oligosaccharides by microbore high-performance liquid chromatography. *Anal. Chem.* **2000,** *72*, 1469–1474.
22. Charlwood, J.; Birrell, H.; Gribble, A.; Burdes, V.; Tolson, D.; Camilleri, P. A probe for the versatile analysis and characterization of N-linked oligosaccharides. *Anal. Chem.* **2000,** *72*, 1453–1461.
23. Naven, T. J. P.; Harvey, D. J. Cationic derivatization of oligosaccharides with Girard's T reagent for improved performance in matrix-assisted laser desorption/ionization and electrospray mass spectrometry. *Rapid Commun. Mass Spectrom.* **1996,** *10*, 829–834.
24. Zhao, Y.; Kent, S. B. H.; Chait, B. T. Rapid, sensitive structure analysis of oligosaccharides. *Proc. Natl. Acad. Sci. (USA)* **1997,** *94*, 1629–1633.
25. Harvey, D. J. Collision-induced fragmentation of underivatised carbohydrates ionized by electrospray. *J. Mass Spectrom.*, in press.
26. Domon, B.; Costello, C. E. A systematic nomenclature for carbohydrate fragmentations in FAB-MS/MS spectra of glycoconjugates. *Glycoconjugate J.* **1988,** *5*, 397–409.
27. Orlando, R.; Bush, C. A.; Fenselau, C. Structural analysis of oligosaccharides by tandem mass spectrometry: Collisional activation of sodium adduct ions. *Biomed. Environ. Mass Spectrom.* **1990,** *19*, 747–754.
28. Spengler, B.; Kirsch, D.; Kaufmann, R.; Lemoine, J. Structure analysis of branched oligosaccharides using post-source decay in matrix-assisted laser desorption/ionization mass spectrometry. *J. Mass Spectrom.* **1995,** *30*, 782–787.
29. Lemoine, J.; Fournet, B.; Despeyroux, D.; Jennings, K. R.; Rosenberg, R.; De Hoffmann, E. Collision-induced dissociation of alkali metal cationized and permethylated oligosaccharides: influence of the collision energy and of the collision gas for the assignment of linkage position. *J. Am. Soc. Mass Spectrom.* **1993,** *4*, 197–203.
30. Harvey, D. J.; Bateman, R. H.; Green, M. R. High-energy collision-induced fragmentation of complex oligosaccharides ionized by matrix-assisted laser desorption/ionization mass spectrometry. *J. Mass Spectrom.* **1997,** *32*, 167–187.
31. Zhou, Z.; Ogden, S.; Leary, J. A. Linkage position determination in oligosaccharides: MS/MS study of lithium–cationised carbohydrates. *J. Org. Chem.* **1990,** *55*, 5444–5446.
32. Hofmeister, G. E.; Zhou, Z.; Leary, J. A. Linkage position determination in lithium-catonised disaccharides: tandem mass spectrometry and semiempirical calculations. *J. Am. Chem. Soc.* **1991,** *113*, 5964–5970.
33. Gillece-Castro, B. L.; Burlingame, A. L. Oligosaccharide characterization with high-energy collision-induced dissociation mass spectrometry. *Methods Enzymol.* **1990,** *193*, 689–712.
34. Reinhold, V. N.; Reinhold, B. B.; Costello, C. E. Carbohydrate molecular weight profiling, sequence, linkage and branching data: ES-MS and CID. *Anal. Chem.* **1995,** *67*, 1772–1784.
35. Patel, T.; Bruce, J.; Merry, A.; Bigge, C.; Wormald, M.; Jaques, A.; Parekh, R. Use of hydrazine to release in intact and unreduced form both N- and O-linked oligosaccharides from glycoproteins. *Biochemistry* **1993,** *32*, 679–693.
36. Prime, S. B.; Shipston, N. F.; Merry, T. H. Enzymatic sequence analysis of glycoprotein glycans. *BioMethods* **1997,** *9*, 235.
37. Harvey, D. J. Quantitative aspects of the matrix-assisted laser desorption mass spectrometry of complex oligosaccharides. *Rapid Commun. Mass Spectrom.* **1993,** *7*, 614–619.
38. Mo, W. J.; Takao, T.; Sakamoto, H.; Shimonishi, Y. Structural analysis of oligosaccharides derivatized with 4-aminobenzoic acid 2-(diethylamino)ethyl ester by matrix-assisted laser desorption/ionization mass spectrometry. *Anal. Chem.* **1998,** *70*, 4520–4526.
39. Fu, D.; Chen, L.; O'Neill, R. A. A detailed structural characterization of ribonuclease B oligosaccharides by 1H NMR spectroscopy and mass spectrometry. *Carbohydrate Res.* **1994,** *261*, 173–186.
40. Harvey, D. J.; Naven, T. J. P.; Küster, B.; Bateman, R. H.; Green, M. R.; Critchley, G. Comparison of fragmentation modes for the structural determination of complex oligosaccharides ionized by matrix-assisted laser desorption/ionization mass spectrometry. *Rapid Commun. Mass Spectrom.* **1995,** *9*, 1556–1561.
41. Harvey, D. J.; Wing, D. R.; Küster, B.; Wilson, I. M. Post-source decay fragmentation of N-linked carbohydrates from ovalbumin and related glycoproteins. *J. Am. Soc. Mass Spectrom.* **2000,** *11*, 572–577.
42. Yamashita, K.; Kammerling, J. P.; Kobata, A. Structural study of the carbohydrate moiety of hen ovomucoid: occurrence of a series of pentaantennary complex-type asparagine-linked sugar chains. *J. Biol. Chem.* **1982,** *257*, 12809–12814.
43. Yamashita, K.; Kammerling, J. P.; Kobata, A. Structural studies of the sugar chains of hen ovomucoid: Evidence that they are formed mainly by the alternate biosynthetic pathway of asparagine-linked sugar chains. *J. Biol. Chem.* **1983,** *258*, 3099–3106.
44. Da Silva, M. L. C.; Stubbs, H. J.; Tamura, T.; Rice, K. G. ^{1}H-NMR characterization of a hen ovalbumin tyrosinamide N-linked oligosaccharide library. *Arch. Biochem. Biophys.* **1995,** *318*, 465–475.
45. Cancilla, M. T.; Penn, S. G.; Carroll, J. A.; Lebrilla, C. B. Coordination of alkali metals to oligosaccharides dictates fragmentation behavior in matrix assisted laser desorption ionization/Fourier transform mass spectrometry. *J. Am. Chem. Soc.* **1996,** *118*, 6736–6745.
46. Harvey, D. J. *N*-[2-Diethylamino)ethyl-4-aminobenzamide derivatives for high sensitivity mass spectrometric detection and structure determination of N-linked carbohydrates. *Rapid Commun. Mass Spectrom.* **2000,** *14*, 862–871.
47. Cancilla, M. T.; Wong, A. W.; Voss, L. R.; Lebrilla, C. B. Fragmentation reactions in the mass spectrometry analysis of neutral oligosaccharides. *Anal. Chem.* **1999,** *71*, 3206–3218.
48. Naven, T. J. P.; Harvey, D. J. Effect of structure on the signal strength of oligosaccharides in matrix-assisted laser desorption/ionization mass spectrometry on time-of-flight and magnetic sector instruments. *Rapid Commun. Mass Spectrom.* **1996,** *10*, 1361–1366.
49. Powell, A. K.; Harvey, D. J. Stabilisation of sialic acids in N-linked oligosaccharides and gangliosides for analysis by positive ion matrix-assisted laser desorption-ionization mass spectrometry. *Rapid Commun. Mass Spectrom.* **1996,** *10*, 1027–1032.